First International Conference on Damage Tolerance of Aircraft Structures
R. Benedictus, J. Schijve, R.C. Alderliesten, J.J. Homan (Eds.)

CALCULATION OF STRESS INTENSITY FACTORS OF CRACKED T-JOINTS CONSIDERING LASER BEAM WELDING RESIDUAL STRESSES

George N. Labeas* and Ioannis D. Diamantakos

*Laboratory of Technology & Strength of Materials, University of Patras,
Panepistimioupolis, Rion, 26500, Greece
e-mail: labeas@mech.upatras.gr
Web page: www.mech.upatras.gr/~ltsm

Abstract. *A damage tolerance analysis methodology for Laser Beam Welded (LBW) structures is proposed. The Residual Stresses (RS) of LBW T-joints are initially calculated through the thermo-mechanical simulation of the LBW process. Through cracks of variable length are considered near the weld and the calculated RS field is introduced in the numerical calculation of the Stress Intensity Factors (SIF). As the Finite Element (FE) models used for the thermo-mechanical simulation can not be the same to those required for the fracture analysis, a special numerical routine based on interpolation techniques is applied for the transfer of RS field to the fracture mechanics FE model. The computation of SIFs at the crack front is performed for mode-I external loading. The RS effect of various cracked T-joint configurations on the SIF values at different through-the-thickness locations is studied. It is shown that both the RS field, as well as the other studied parameters, has a significant influence on the Stress Intensity Factors.*

1 INTRODUCTION

Laser Beam Welding (LBW) technology has recently attracted the interest of aircraft and other manufacturers, mainly due to increased productivity and low effect on the local material properties. A challenging application of LBW is the connection of stiffener and frame clips to the skin of aircraft fuselage, using T-type joints. However, LBW leads to the development of Residual Stresses (RS) and distortions[1-3], which change the stress field in the vicinity of the weld and affect significantly the crack generation and propagation rate. In general, the RS field reduces the structural integrity and fatigue life of the structure[4]; therefore, the RS field has to be taken into account in the assessment of damage tolerance behaviour of welded structures.

The basic mechanism of RS generation results from high temperatures and high temperature gradients developed during the laser pass, which lead to large local thermal expansion of the material; the adjacent material tends to resist this expansion leading to local plastic deformation and RS development. Several analytical[1, 5-6] and numerical[7-13] models have been proposed for the prediction of temperature, RS and distortions history during LBW process. However, most of the simulated welding cases concern butt-joints, while more complex geometries (e.g. T-joints) have not been treated. Moreover, most of the studies refer to steel structures, while investigations on typical aerospace Aluminium joints are quite

limited.

A common methodology for assessing the behaviour of cracked structures, with or without RS, is the SIF approach. Limited works have been published for the calculation of SIFs under RS fields. Tada et al.[14] and Terada[15-16] have used a customary method based on the superposition principle and Muskhelishvili's stress functions for the calculation of SIFs at through cracks situated perpendicular to the welding bead. However, refs [14-16] refer to the influence of one-dimensional RS fields on the SIFs of through cracks, ignoring the RS variation through-the-thickness, which is not realistic in practical applications and does not always represent the most critical situation.

In the present work, the effect of realistic RS fields, as calculated via a thermo-mechanical LBW simulation, on the SIF values at crack front is studied. A parametric investigation considering various T-joint geometrical details is performed. The thermo-mechanical model considers all the physical phenomena occurring during the welding process, e.g. heat transfer via conduction, convection and radiation, melting, solidification etc. Thermal and mechanical material properties are introduced as temperature-dependent functions. The model is verified by the comparison of numerical results to RS measurements from respective experiments. Through cracks of variable lengths are considered near the weld and proper three-dimensional FE models are developed for the fracture analysis of the cracked structures. As the FE discretization of the thermo-mechanical model should be different from that required for the fracture mechanics model, a special numerical routine based on interpolation methods is applied for the RS transfer. The solution of the fracture mechanics model for mode-I external loading results to SIF computation at the crack front. It is shown that the presence of RS has a serious influence on the SIF values.

2 CALCULATION OF RESIDUAL STRESS FIELD

2.1 T-joint configurations studied

The proposed damage tolerance methodology taking into account LBW residual stresses is applied in the case of the skin-clip T-joint configuration, presented in Figure 1. A 2mm thick Al-6013 clip is welded to a 6mm thick Al-6056 skin. Three variations of the T-joint are considered, i.e. no pockets in the skin, pockets of 2mm depth and pockets of 4mm depth.

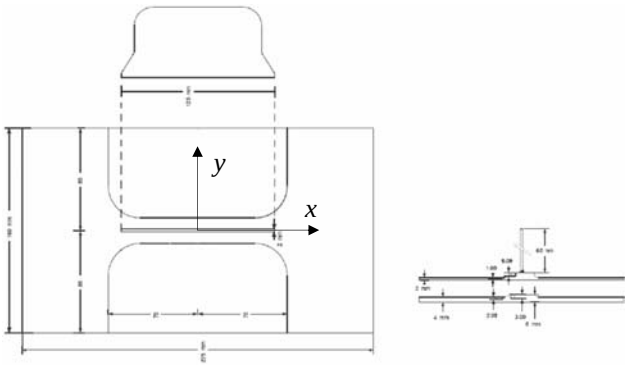

Figure 1: Geometry of the skin-clip specimen with milled pocket

The weld is conducted using a CO_2 laser of 3.3 kW, 1.8 $^{m}/_{min}$ welding velocity, 20^{o} welding angle with respect to the skin and Al-4047 filament wire of 1.2mm diameter.

2.2 LBW simulation methodology

The main steps of LBW simulation methodology are presented in the flow-chart of Figure 2 [17]. The same FE model is used for both the thermal and mechanical analyses. A transformation of thermal elements used for the thermal analysis to structural ones used for the mechanical analysis is performed.

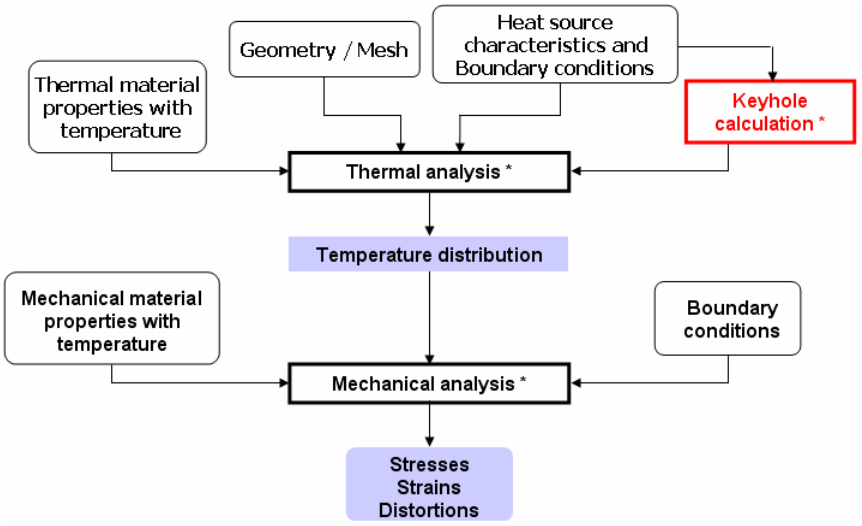

Figure 2: Flow chart of LBW process simulation methodology, after [17]

The thermo-mechanical FE model (see Figure 3) comprises about 75000 three-dimensional elements and has very dense mesh in the area along and nearby the weld line, as high temperature and stress gradients develop in this area.

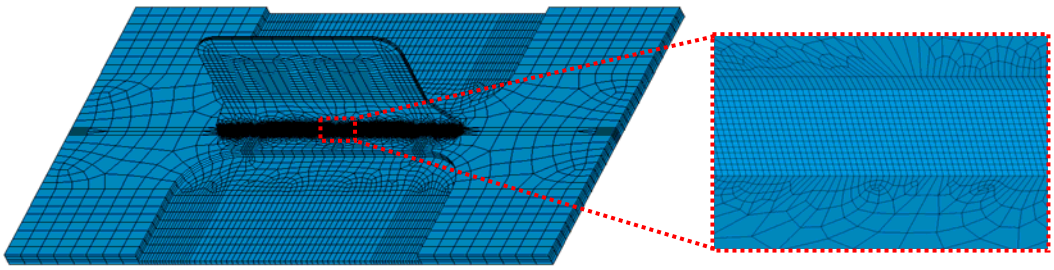

Figure 3: Thermo-mechanical FE model

A comparison between numerical RS predictions and experimental measurements are presented in Figure 4. The experimental T-joint RS results are taken from [18] and refer to the mid-thickness of the skin at the x, y, z directions; a good correlation is observed between the experimental and numerical results.

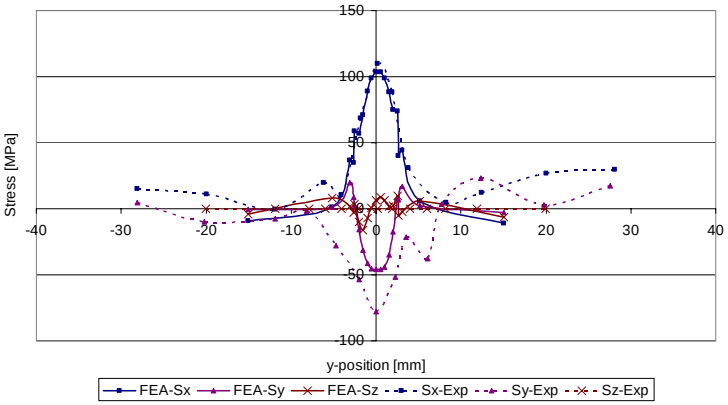

(a)

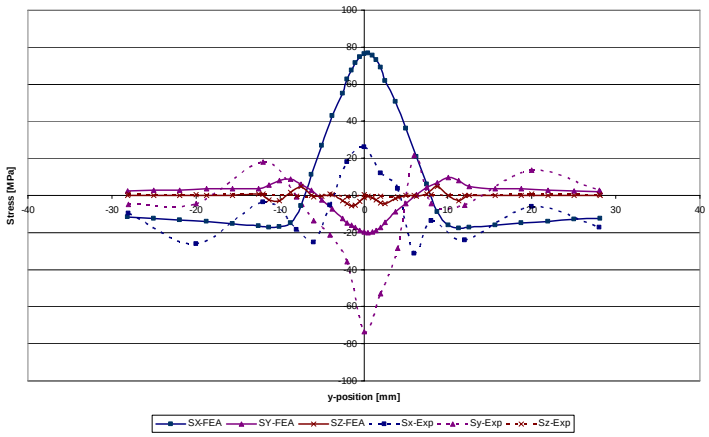

(b)

Figure 5: Comparison between experimental and computed RS results at mid-skin, (a) plate without pockets and (b) plate with pockets of 4 mm depth.

3 ANALYSIS OF CRACKED T-JOINTS

3.1 Description of the fracture mechanics model

A through crack of half-length varying from 5 to 35mm, parallel to the weld, located 7 mm from the plate centre is considered at the T-joint. For the SIF calculation a three-dimensional model of the cracked structure, comprising about 40000 ‘SOLID95’ elements of ANSYS FE code and 160000 nodes is developed, see Figure 5. The most critical region is around the crack edge, as the displacements near the crack front vary as $r^{1/2}$, where r is the distance from the crack front. The stresses and strains are singular at the crack tip, varying as $r^{-1/2}$. In order to enable simulation of this singularity, singular elements, which have their mid-side nodes placed at the quarter points are used, forming a “spider-web” mesh pattern, as shown in the detail of Figure 5.

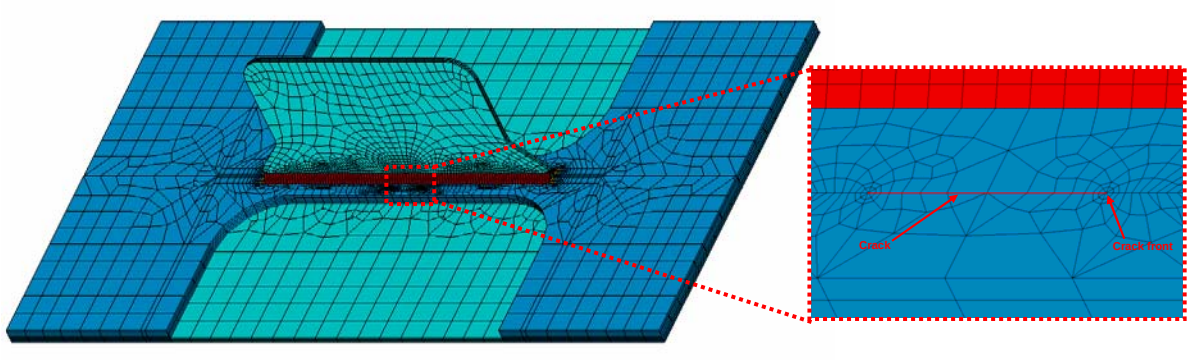

Figure 5: Fracture mechanics model of T-joint structure

The remote load at the edge of the plate is applied perpendicular to the clip and corresponds to a mean stress of 100 MPa at the middle of the plate (considering skin thickness without pockets). The plate is clamped at the one edge. At the other edge all movements are constrained, except the one at the direction of the loading; additionally, coupled degrees of freedom are defined for these nodes, in order to force them to move all together at the direction of the external load.

3.2 Residual stresses transfer method

As mentioned above, residual stresses due to the LBW process, as calculated by the numerical thermo-mechanical simulation, have to be introduced in the fracture mechanics analysis. However, the thermo-mechanical FE model (Figure 3) used for the simulation of LBW process model is significantly different from the fracture mechanics one (Figure 5), because:

(a) The mesh density and pattern requirements are different for LBW simulation and fracture analysis. For the case of LBW simulation, high mesh density is required at the area of welding. An adequate number of elements, usually of about 0.1mm size, must be used for modelling the local volume directly affected by the laser beam. On the other hand, the proper mesh of the fracture mechanics model must have high concentration of elements, usually of about 0.1mm size, in the crack front location.

(b) The results of one thermo-mechanical simulation may be used for the fracture mechanics analysis of several crack configurations (e.g. different crack lengths, locations and orientations).

The RS transfer between the two different FE models is performed using a special routine, which is based on the interpolation kit-tool of MATLAB software. The RS to be applied at the element centroids of the fracture mechanics model are interpolated by the computed RS values at the nodal positions of the thermo-mechanical model. Calculated residual stresses are applied as initial stresses at the FE model used for the analysis of cracked T-joints.

3.3 Effect of RS and T-joint geometry on computed SIFs

Linear static stress analysis leads to the computation of SIFs at the crack fronts for cracks developing in the three T-joint configurations described above and for various crack lengths. This analysis uses a fit of the nodal displacements in the vicinity of the crack for the computation of the corresponding SIF. SIF value is not constant in the crack front, but varies from the top to the bottom of the plate, due to the through-the-thickness variation of RS field and the asymmetry of the geometry. Thus, SIFs are also calculated for various "depths", from 0 mm (top of the plate) to 6 mm (bottom of the plate). The effect of RS field, T-joint geometry (i.e. depth of pocket) on the calculated SIFs has been studied

In Figure 6, the calculated SIFs with and without the residual stress field are plotted for the various T-joint configurations and crack lengths for three different locations at the crack front; top, middle and bottom of plate.

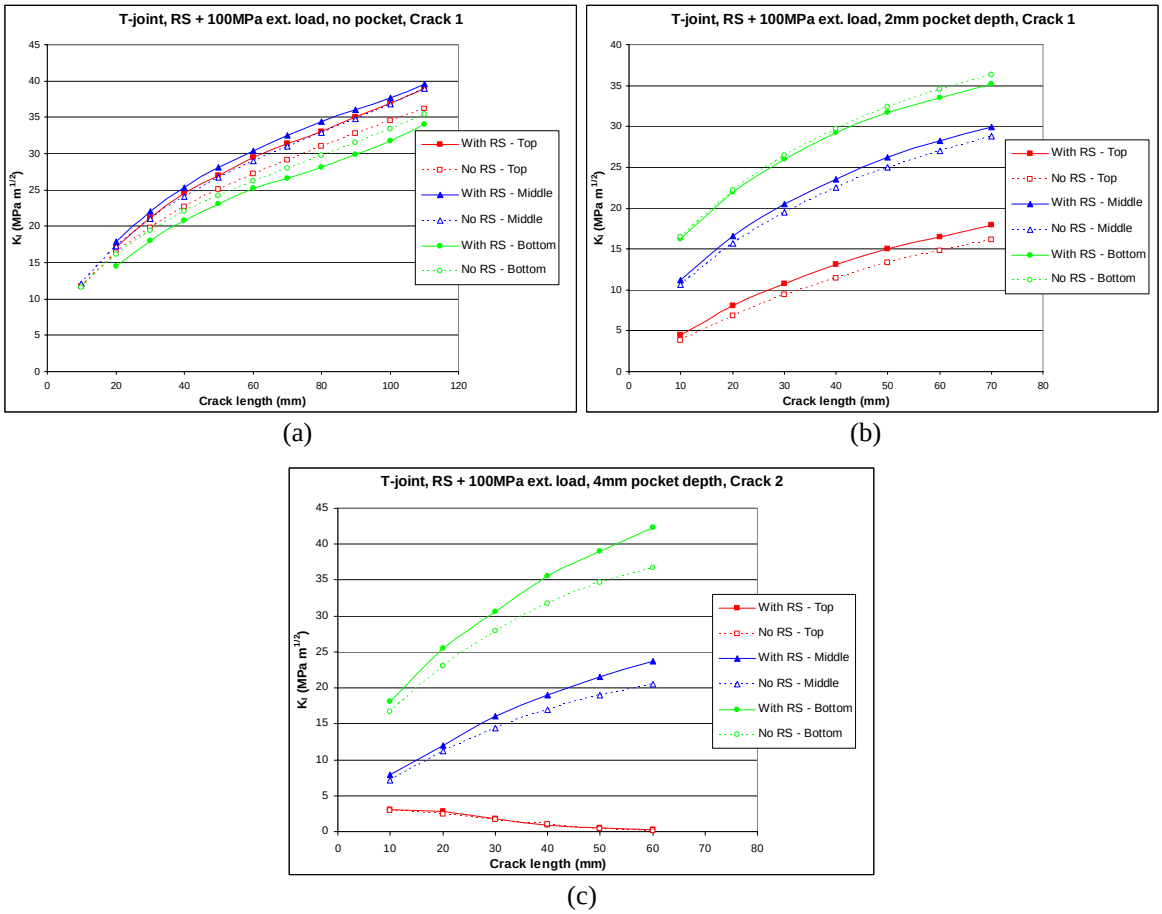

Figure 6: Calculated SIFs with and without residual stresses at the top, middle and bottom of crack front, (a) T-joint without pockets, (b) pockets of 2mm and depth (c) pockets of 4mm depth.

The effect of T-joint geometry (i.e. pocket depth) on the calculated SIFs may be observed in the diagrams of Figure 7. Additionally, in order to examine whether the calculated values

are mainly influenced by the residual stresses or by the T-joint geometry the diagrams of Figure 7 are repeated in Figure 8 without taking into account the RS field.

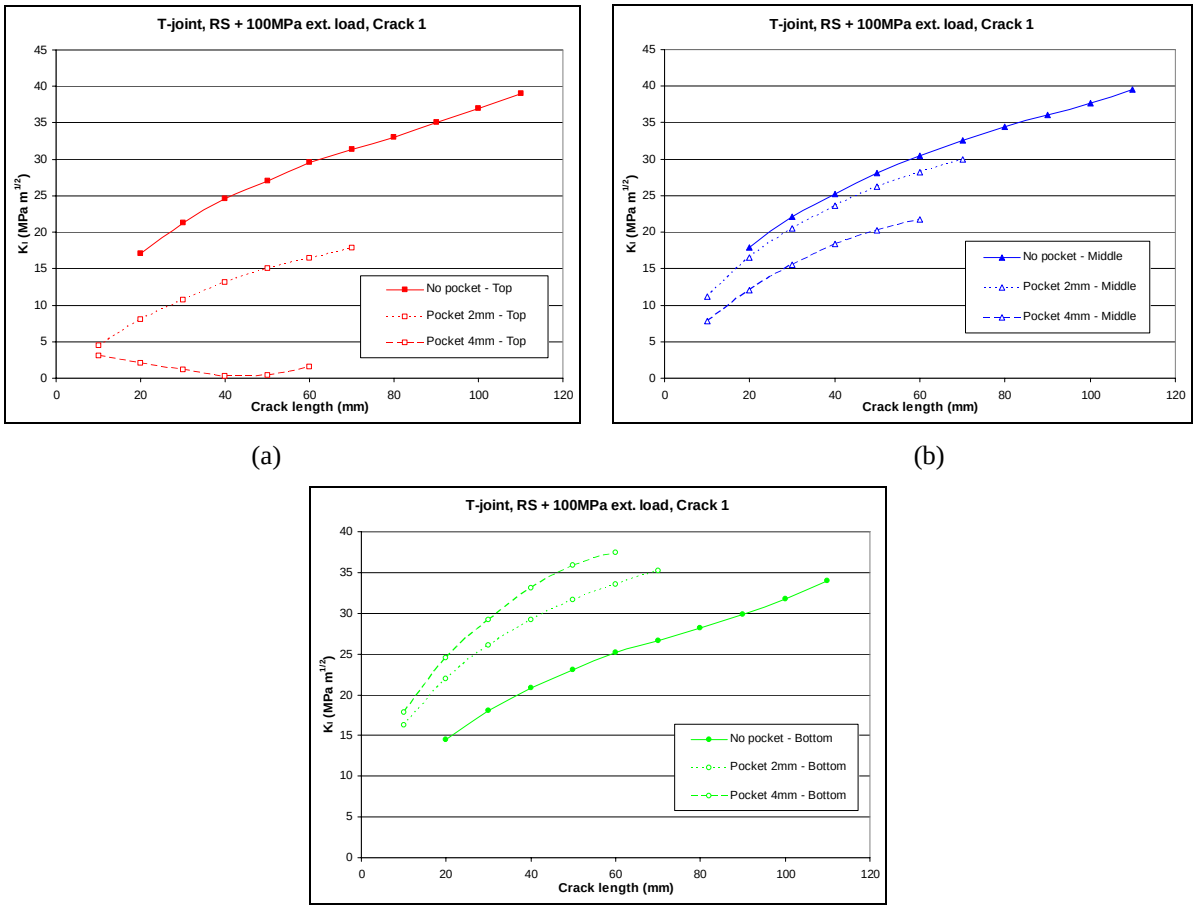

Figure 7: Effect of plate geometry on the calculated SIFs taking into account residual stresses and external load. (a) top of plate, (b) middle of plate and (c) bottom of plate

4 CONCLUSIONS

The effect of RS on the calculated SIFs may be summarised as following:

a) RS lead to an increase of the calculated SIFs at the middle of the crack fronts.
b) For the point of the crack front situated at the top of the plate RS lead to increase of the calculated SIFs for the cases of the plate without pocket and with pockets of 2mm depth. For the case of the T-joint with pockets of 4mm depth the effect is not clear. It has to be mentioned that for this case the SIFs at the top of the crack front are relatively low, possibly due to the bending of the joint that leads to closure of the crack lips.

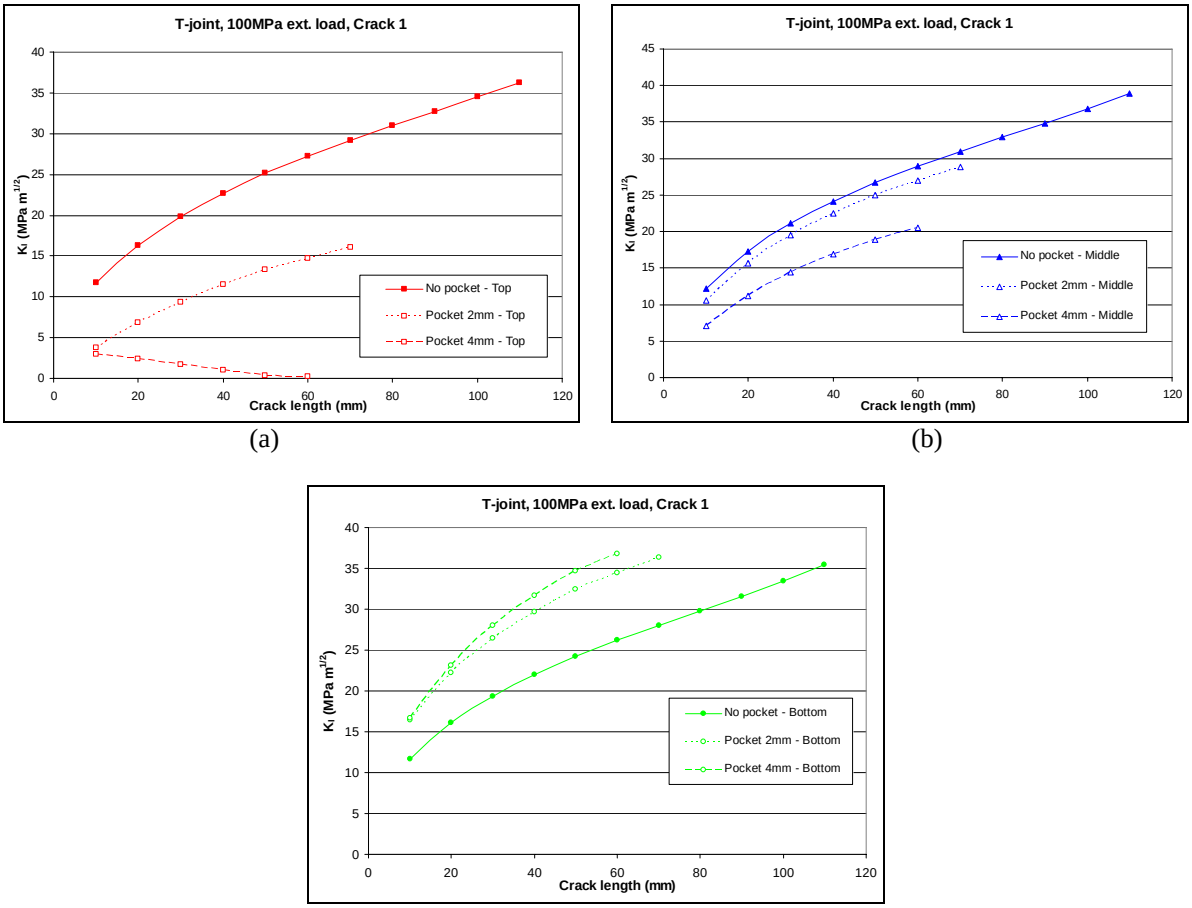

Figure 8: Effect of plate geometry on the calculated SIFs taking into account only external applied load. (a) top of plate, (b) middle of plate and (c) bottom of plate

c) For the point of the crack front situated at the bottom of the plate the effect of residual stresses on the calculated SIFs is not clear, but it depends on the specific case characteristics. For the case of the plate with 2mm deep pocket SIFs decrease with the presence of residual stresses. Finally, for the case of the plate with 4mm deep pocket residual stresses leads to a SIFs increase.

The effect of T-joint geometry on the calculated SIFs may be summarized as following:

a) For the point of the crack front situated at the top of the plate a dramatic decrease on the calculated SIFs is observed with increase of pocket depth. This may be attributed to the bending of the clip, due to the asymmetry of the clips that leads to closure of crack lips.
b) For the point of the crack front situated at the middle of the plate the increase of pocket depth leads to a moderate decrease on the calculated SIFs. This may be due to the smaller effect of bending to the deformations of the middle of crack front.
c) The effect of pocket depth on the SIFs is the inverse for the point at the bottom of the crack front. The increase of pocket depth leads to increase of the calculated SIFs at the

specific point. This observation may also be attributed to the bending of the joint, as it leads to further opening of crack lips.

d) The variations at the T-joint geometry have the same major effect on the calculated SIFs even if the RS are neglected. This may be attributed to the fact that the considered crack is situated near the pocket and thus it is heavily influenced by bending caused by the asymmetry of the geometry.

ACKNOWLEDGEMENTS

Part of this work was performed in the frame of the European Research Programme "Development of short distance WELding concepts for AIRframes" (WEL-AIR). The financial support of the European Union under contract AST3-CT-2003- 502 832 is gratefully acknowledged. The LBW experiments were conducted by GKSS, in the frame of research activities of the above referred project.

REFERENCES

[1] L. J.Yang, Z. M. Xiao, "Elastic-plastic modelling of the residual stress caused by welding", J. Mat. Proc. Techn., 48, 589-601, (1995).

[2] K. Masubuchi., *Analysis of welded structures*, Pergamon Press, Oxford, UK (1980).

[3] S. A.Tsirkas, P. Papanikos, Th.Kermanidis, Numerical simulation of the laser welding process in butt-joint specimens", J. of Mater. Process. Technol., Vol.134, 59-69, (2003).

[4] Dalle Donne, C., Biallas, G., Ghidini, T., Raimbeaux, G, In: Second International Conference on Friction Stir Welding, TWI, Abington Hall, (2000).

[5] N. Okerblow, *The calculations of deformations of welded metal structures*, Her Majesty's Stationery Office, London UK, (1958).

[6] Y. Tanigawa, T. Akai, R. Kawamura, N. Oka, Transient Heat Conduction and Thermal Stress Problems of a Nonhomogeneous Plate with Temperature-Dependent Material Properties, Journal of Thermal Stresses, 19, 77-102, (1996).

[7] Cho, S.-K., Yang, Y.-S., Son, K.-J. and Kim, J.-Y., (2004), Finite Elem Anal Des, 40, 1059–1070.

[8] Chakravarti, L. M. Malik, and J. Goldak, "Prediction of Distortion and Residual Stresses in Panel Welds", In computer modeling of fabrication processes and constitutive behavior of metals, Ottawa, Ontario, Canadian Government Publishing Centre, 1986, 547-561.

[9] S. Fujii, N. Takahashi, S. Sakai, T. Nakabayashi and M. Muro, Development of 2D Simulation Model for Laser Welding, Proceedings of SPIE, Vol. 3888, 2000.

[10] M. R. Frewin, D. A. Scott, Finite Element Model of Pulsed Laser Welding, Welding Journal, Welding Research Supplement, 15s-22s, (1999).

[11] G. Reinhart, B. Lenz, F. Rick, Finite Element Simulation for the Planning of Laser Welding Applications, Proc. Of the 18th intern. Congress on Applications of Lasers & Electro-Optics (ICALEO'99), San Diego/CA, (1999).

[12] C. Carmignani, R. Mares, G. Toselli, Transient finite element analysis of deep penetration laser welding process in a single-pass butt-welded thick steel plate, Comput. Methods Appl. Mech. Engrg., 179, 197-214, (1999).

[13] D.-H. Kang, K.-J. Son, Y.-S. Yang, Analysis of laser weldment distortion in the EDFA LD pump packaging, Finite Elements in Analysis and Design, 37, 749-760, (2001).
[14] H. Tada, P.C. Paris, “The stress intensity factor for a crack perpendicular to the welding bead”, Int. J. Fracture, 21, 279–284, (1982).
[15] H.Terada, “An analysis of the stress intensity factor of a crack perpendicular to the welding bead”, Eng. Fract. Mech., 8, 441-444, (1976).
[16] H. Terada, and T. Nakajima, “Analysis of stress intensity factor of a crack approaching welding bead”, Int. J. Fracture, 27, 83-90, (1985).
[17] G. Moraitis and G. Labeas, ‘‘Residual Stress and Distortion Calculation of Laser Beam Welding for Aluminum Lap joint Journal of Materials Processing Technology’’, accepted for publication in J. Mater. Proc. Techn.
[18] F.S. Bayraktar, P. Staron, M. Kocak, A. Schreyer, ”Residual stress analysis of Laser Welded Aluminium T-Joints Using Neutron Diffraction”, 7th European Conference on Residual Stresses, Berlin, 13-15 September 2006.